Responses to Referee#2 (Steffen Beirle) comments and appendix A:

The study "Benchmarking data-driven inversion methods for the estimation of local CO2 emissions from XCO2 and NO2 satellite images" investigates the performance of various approaches for the quantification of CO2 emissions from synthetic satellite images. As the quantification of CO2 emissions from upcoming satellites is a very important task with strong political and economical impact, this study provides an important scientific contribution. The study is generally well written, and matches the cope of AMT. However, I see one of the main results of this study, i.e. the rather poor performance of the divergence method, related to the way this method was implemented (temporal mean only), which is quite different from for treatment of the other methods (single images). I thus recommend publication after dealing with the comments below.

Thank you for your positive comments. We agree that focusing on a version of the divergence method which provides temporal mean fluxes only in the comparison to the other methods, which also provide single image estimates, can be questioned. However, the overarching goal of our paper is to benchmark data-driven methods in their current standard versions, i.e. in the most common way they are used. And, the different versions of the divergence method that have been studied in recent years provide temporal-averaged (mostly annual) emissions (Beirle et al., 2019, 2021; Hakkarainen et al., 2022, Sun, 2022). To our knowledge, there is a lack of study on the use of the divergence method to estimate instant emissions from single satellite images, and thus of knowledge about how to adapt this method for such an application. This explains why we had to conduct a series of sensitivity experiments to properly address the following comments, as detailed below.

Actually, a second reason for which we did not investigate the application of the divergence method to estimate emissions from single overpasses in the first version of our manuscript was that the first insights from the analysis of divergence maps suggested that they were unusable for this purpose: these maps extracted from single images can indeed show important variabilities as shown by the example of the strong emitting power plant of Janschwalde for January 12 (Figs R1, R2). This and other examples suggested that the computation of the emissions from single divergence maps using direct integration lacks reliability when applied to this type of data. Our parallel analysis on TROPOMI SO2 data (not documented in this study) strengthened this assumption, suggesting that the problem was not specific to the application to the SMARTCARB dataset, but likely a methodological limitation of the divergence approach based on the spatial integration of the divergence signal (called hereinafter *integral* divergence approach): small changes in the integration radius could lead to large changes in the estimated emissions suggesting that this approach was not very robust, as shown in the example of the figure R1.

This is why, in the first version of the manuscript, we chose the peak fitting approach to extract the emissions from the divergence map instead of integrating the divergence signal (Beirle et al., 2019, 2023). This approach works better with noisy

data thanks to the natural smoothing effect of the bivariate Gaussian function and provides relatively accurate annual estimates as shown in our study. However, its application to individual overpasses raises challenges. Proper and nice peaks are rarely visible in CO2 divergence maps extracted from individual images. Attempting to fit the data with the peak model often yields poor results both visually and in terms of emission estimates; the divergence map around a source hardly fits with a "peak"-like shape. This is the case for the example in Figures R1 and R2 where the determination of the parameters of the Gaussian bivariate function does not converge. The peak-fitting approach may also attempt to fit false plumes if the divergence from a given source is not strong enough or because there are numerical artifacts in the divergence map close to the source.

Our explanation for the lack of robustness of the divergence approaches when applied to single CO2 images that was suggested by this analysis lied on:

(1) the fact that we do not compute the divergence method perfectly in line with the theory. For example, as can be seen in Figure 7 of Koene et al. (2024, https://doi.org/10.1029/2023JD039904), the divergence flux map for a plume is *never* merely a simple enhancement at the source and "zero" elsewhere. There are too many violations of assumptions, e.g., that the effective wind field is perfect. Integration of the divergence flux map thus starts capturing features that are not related to source emissions at all.

(2) the presence of other (CO2) sources and sinks, meaning that a different radius selects additional but unwanted sources/sinks.

We illustrate graphically the benefit of averaging the divergence maps, using, again, results for the Janschwälde power plant. The annual averaged divergence map in the area of this power plant is given in Figure R3. In this example, the enhancement over the background is much closer to a 2D Gaussian shape and the estimate by the peak-fitting divergence approach was found to be ~44.9 MtCO2/yr. This estimate of the annual emissions is indeed close to the true value (~41.5 MtCO2/yr). The integrated divergence method also generated good results: 36.6, 46.3 and 46.3 MtCO2/yr for an integration radius of 3, 5, and 7 km respectively.

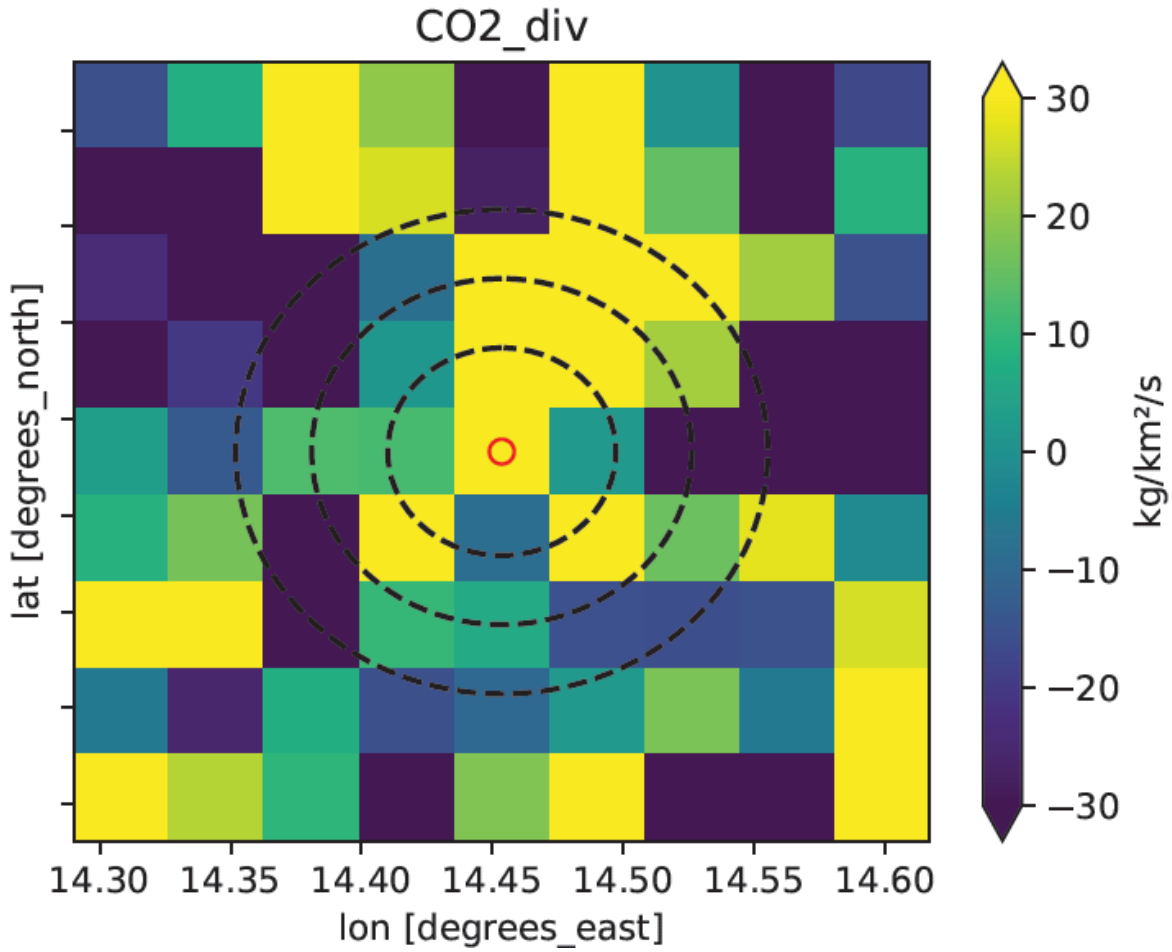

Figure R1: Divergence map estimated around the Janschwalde power station on January 2015 the 12th. Dotted circles show the different integration radii (3 km, 5 km and 7 km) used by the divergence method when emissions are derived from the integration of the divergence maps. Estimates are about 60.3, 111.2 and 120.2 MtCO2/yr when using integration radii 3, 5, and 7 km respectively. The true value being 52.2 MtCO2/yr, this suggests that the integrated divergence approach generates uncertain results which strongly depends on the integration radius when inverting single images. The peak-fitting divergence approach was not able to produce any result because it was unable to fit a Gaussian bivariate function to the divergence map.

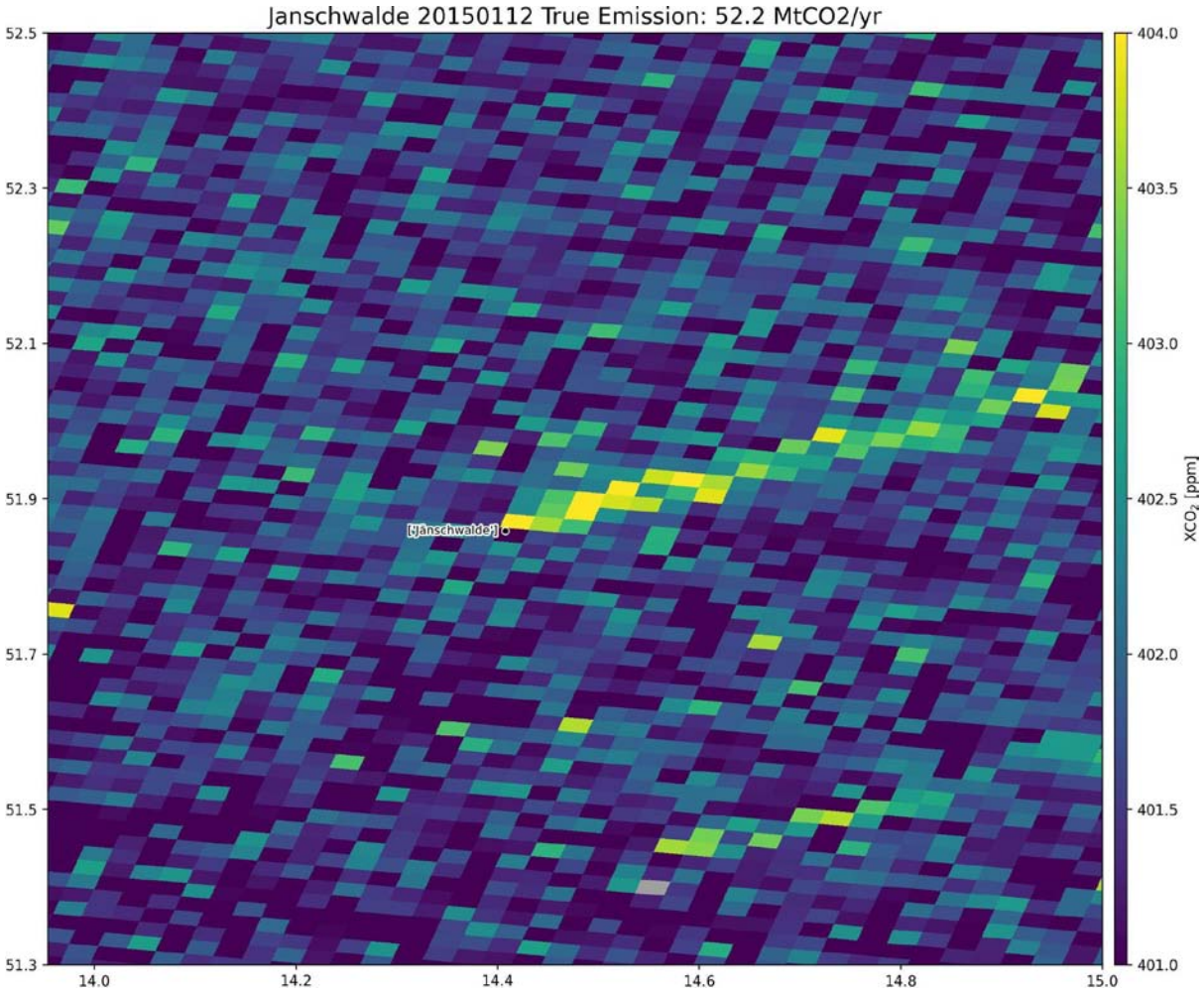

Figure R2: XCO2 map (ppm) around the Janschwalde power station on January 2015 the 12th.

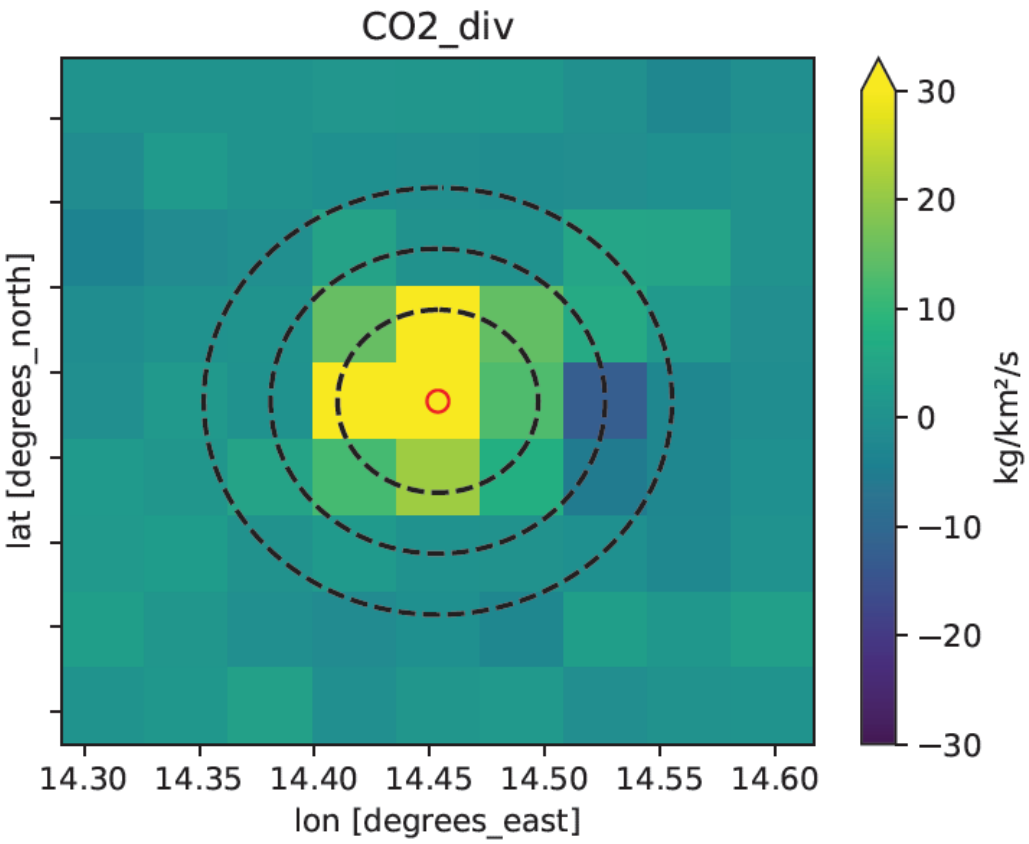

I

Figure R3: Map of the annual average divergence around the Jänschwalde power station for 2015

However, following this review, we have implemented the suggestions made by the referee and retrieved emission estimates from single images using several versions of the divergence approach. These versions compute the divergence maps by considering only the advective term of the divergence expression (see section 3.5 in Beirle et al., 2023) which removes the impact of the background. The results when considering one year of single overpass images showed that the performance of the integral divergence approach is much better than the peak-fitting divergence approach. This led us to conduct an extensive set of computations, varying the integration radius when applying this approach. This finally revealed that, with integration radii close to the spatial resolution of the data, the performance of the integral divergence approach can get comparable to that of the other methods in our study (Figure R4 and R5).

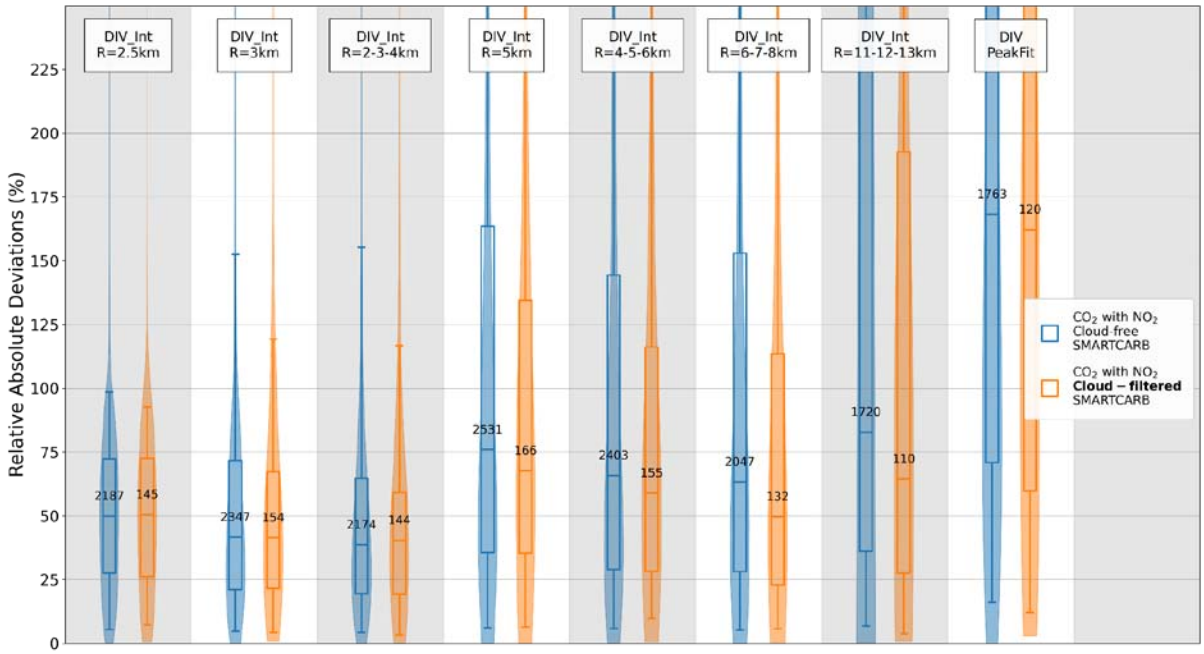

Figure R4: Performances of the different versions of the divergence inversion method when estimating emissions from one year of single images for different benchmarking scenarios: cloud-free CO_2 and NO_2 data with SMARTCARB winds (in blue) and cloud-filtered CO_2 and NO_2 data with SMARTCARB winds (in orange). Distributions of the relative absolute deviations are illustrated using violin plots. Boxes are the inter-quartiles of the distributions, the whiskers are the 5^{th} and 95^{th} percentiles, and the lines within boxes are the medians. Numbers in the inter-quartile boxes are the number of estimates for each benchmarking scenario and inversion method. Methods DIV_int_R=xkm and DIV_PeakFit are the integral (for an integration radius of x km) and peak-fitting versions of the divergence approach respectively. For a given overpass and source, the emission estimate of the method DIV_int_R=x-y-zkm is the average of the estimates when integrating over circles of x, y and z km radius around the source.

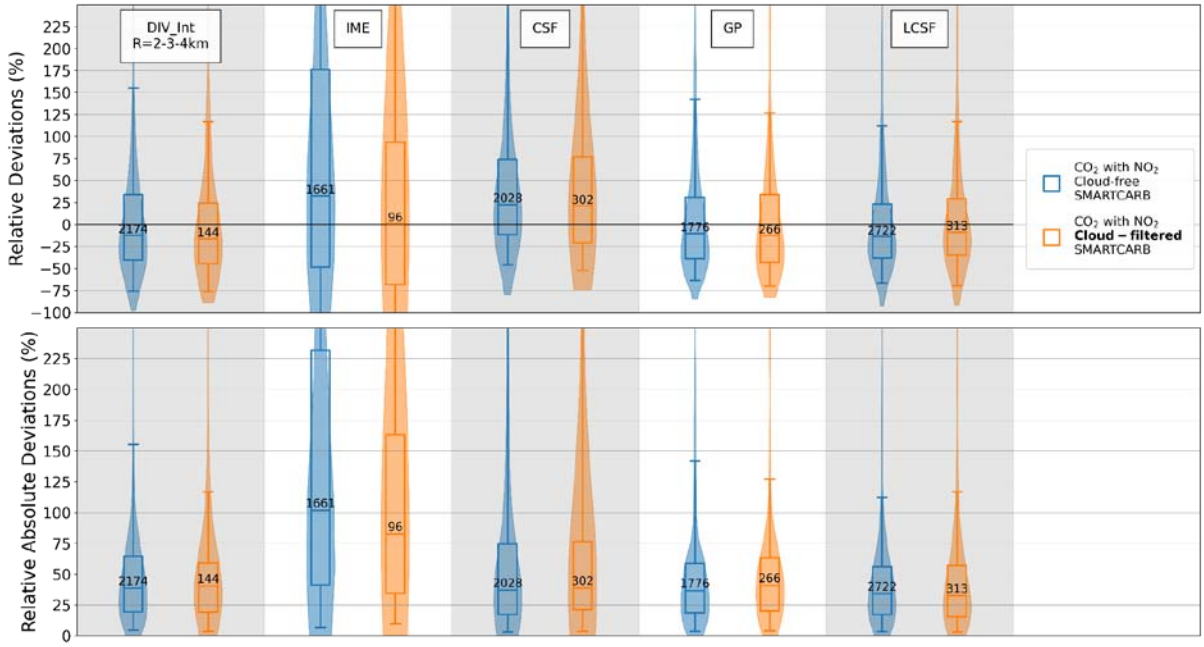

Figure R5: Performances of the inversion methods when estimating emissions from one year of

single images for different benchmarking scenarios: cloud-free CO_2 and NO_2 data with SMARTCARB winds (in blue) and cloud-filtered CO_2 and NO_2 data with SMARTCARB winds (in orange). Distributions of the relative deviations (top panel) and relative absolute deviations (bottom panel) are illustrated using violin plots. Boxes are the inter-quartiles of the distributions, the whiskers are the 5^{th} and 95^{th} percentiles, and the lines within boxes are the medians. Numbers in the inter-quartile boxes are the number of estimates for each benchmarking scenario and inversion method. Methods DIV_int_R=2-3-4km and DIV_PeakFit are the integral and peak-fitting versions of the divergence approach respectively. For a given overpass and source, the emission estimate of the method DIV_int_R=2-3-4km is the average of the estimates when integrating over circles of 2,3 and 4 km radius around the source.

We conclude from this series of reasoning and analysis that:

- We agree with the reviewer that the integral divergence method has a good potential to estimate emissions from single overpasses, comparable to that of the other methods tested in this study. This topic raises very interesting questions
- This deserves some discussion in our manuscript, and a documentation of the new results described here in answer to the review

but

- Fully including the integral divergence method into the comparison of emission estimates based on single images in the main text of the manuscript would require a better analysis of the potential of this approach, and thus some further investigations, which are out of the scope of this study. We managed to get performances comparable to that of the other methods based on a large but non exhaustive set of tests of sensitivity to the integration radius (Fig. R4), while our application of the other methods could rely on configurations from past experiments. Such investigations would include: testing whether the skill of the approach could be further improved by refining the integration radius, identifying why the best results are currently obtained for a radius close to the spatial resolution of the images etc... In addition to deriving meaningful indices of the uncertainties in the corresponding emission estimates.

This adds to our choice to benchmark data-driven inversion methods in standard configurations documented by previous studies.

Therefore, we have decided not to include the results of the divergence method for single-image estimates in the main part of the article, but to discuss them in the conclusion section 6 and to document them in the new Appendix A (see end of this document) as preliminary results. The paragraph inserted in the conclusion section is as follows:

In this study, we chose not to analyze the potential of the divergence method for estimating instant emissions from single satellite overpasses because of the lack of

studies on such an application of this method. As highlighted in the introduction section, our aim is to compare proven approaches for the local scale estimate of strong sources (such as the application of the divergence method to time-averages of satellite images). Moreover, the strong spatial variability of the divergence fields derived from single images suggest that only averaged fields could be processed properly with the version of the divergence approach which is used here for annual estimates and which relies on the peak-fitting of temporally averaged divergence fields. However, we have conducted some preliminary analysis on a version of the divergence method which instead integrates the divergence signal spatially (over disks centered on the sources). The results, documented in appendix A, demonstrate that with a range of integration radii close to that of the spatial resolution of image, this approach can yield estimates that would be comparable in terms of accuracy and quantity to that of the best inversion methods of our benchmark evaluation for single-image based estimates. A better understanding of the behavior of this approach as a function of the integration radius, and an assessment of the estimation errors are needed to conduct a proper comparison to the other methods. This deserves further investigations. However, these preliminary results raise optimistic perspectives regarding the potential of using the divergence method for estimating instant emissions from single-overpass images

In addition to Appendix A and to this new paragraph of the conclusion section, we added some sentences in the section describing the divergence method (section 2.1.5.) in order to mention our choice of applying the divergence method on temporal averaged maps:

Old paragraph:

Divergence maps are computed from flux fields by using a finite difference approximation and in order to clearly detect point sources, the method needs to average the divergence fields over a long period. Here, divergence maps are averaged over one year.

New paragraph:

Divergence maps are computed from the mass flux field using a finite difference approximation. The divergence map is then averaged over a long period to enhance the emission signal, while reducing the impact of noise and the spatio-temporal variations of the CO2 background. Here, divergence maps are averaged over one year. In theory, the divergence method can also be used to estimate emissions from single-overpass images such as the cross-sectional flux method (as the two methods are in theory similar, see Koene et al. 2024). However, we choose in this study to focus on the standard application of this method (e.g., Beirle et al. 2019, 2021, 2023; Hakkarainen et al., 2022, Sun et al., 2022), which provides temporally averaged estimates. Appendix A provides a brief overview of the performance when estimating emissions from individual images with different versions of the divergence approach.

Finally, we mention in the introduction section that the divergence method is, in its standard version, used for inverting temporal-averaged emissions.

Old sentence:

Contrarily to the other methods of this study, the Div method produces annual estimates from average fields extracted from multiple images.

New sentence:

Contrarily to the other methods of this study, the Div method is generally used to generate annual estimates from average fields extracted from multiple images.

Implementation of the divergence method

The authors find the divergence method to show poorest performance for the quantification of CO2 emissions. However, I suspect that this result is partly due to the way the retrieval was done. In particular, the divergence method was treated quite differently, and - if I understood correctly - uses a different data selection then the other methods: The quantification of emissions from methods (1) to (4) require the identification of a plume. I.e. these methods are only applied to favourable conditions which are close to steady state - which is more or less assumed in all approaches. In contrast, the divergence method was applied to a temporal mean flux which probably contains unfavourable conditions as well - please clarify.

We agree with the referee and we have added in the conclusion the sentence: *However, its performance could be improved by selecting and averaging images that are characterized by favorable conditions such as strong signals or wind speeds important enough to guarantee the predominance of advective processes in the atmospheric transport.*

In any case, I don't see why the divergence method is not applied to single images as well as all other methods. For a plume as the one shown in Fig. 1, the divergence of the flux should directly yield the corresponding emissions. The motivation to use a long-term mean in Beirle et al. (2019, 2021, 2023) was that we wanted to *identify* and *localize* point sources first. These tasks are considered as solved in this study - the locations of the considered point sources are given a-priori. Thus the divergence might easily be calculated for the single image data as well, and emissions can be derived by simply integrating the divergence signal within e.g. 15 or 30 km radius around the point source.

We assessed qualitatively the effect of estimating emissions by integrating the divergence signal, using integration radii varying from 3 to 30 kms, for an example similar to the one shown in Fig. 1 of the paper. We found that emissions estimates show an important difference with respect to the true emissions and that they are very sensitive to the chosen integration radius. Probably, as the radius increases,

more and more noisy pixels are included in the integration, yielding varying results depending on the surrounding area. For this reason, estimates corresponding to integration radii greater than 10 km are far from the truth (Fig. R5).

As example, Figure R1 shows the divergence map around the Jänschwalde power plant for January the 12th. Even for this example which is characterized by a “nice” plume in amplitude and shape (Figure R1), the integrated divergence method gives estimates (60.3, 111.2 and 120.2 MtCO2/yr for an integration radius of 3,5 and 7 km respectively) that are very sensitive to the integration radius and in average far from the truth (97 vs 52.2 MtCO2/yr)

The analysis of the example above would suggest that estimating emissions with the integral divergence method from single images is unreliable. However, as discussed above, when analyzing inversion results for a whole year of single images (Figure R5), the performance of the divergence method is much better for a version of the divergence method which averages the estimates derived from the integration of divergence maps for radii of 2,3 and 4 km.

I don't see the need for an a-priori background correction, as the derivative does this automatically.

The divergence method as used in the paper is the "full" divergence method, i.e., ∇ . (VCD*U), while the reviewer undoubtedly expects that the divergence is computed in simplified form as U.∇(VCD). While in the latter expression it is true that a (constant) background is removed by the derivative operation, this does not hold for the “full” divergence method. Then, rather, it really does pay to subtract the background, i.e., to compute ∇.([VCD-BG] * U). A motivation for such an approach has been given in Koene et al. (2024): the effective wind field *U* should only describe the *enhancement* of the CO2 plume – not the total-column density-weighted wind between the surface and the top-of-the-atmosphere. As *U* is typically taken on a fixed model level (e.g., 200 m), not removing the background would mean there is a considerable mis-match between *VCD* (total column) and *U* (wind at one altitude), invalidating the assumptions of the divergence method. By removing the background, we can more safely assume that VCD-BG (the plume enhancement) and U (wind at one altitude) form a consistent data pair. Hakkarainen et al. (2022) showed as well that a background (and noise) removal should be applied to make the divergence method robust for estimating emissions from CO2 data.

However, for the integral divergence methods that have been studied in appendix A, a-priori background correction was indeed found to have a weak impact on the results as we computed the divergence of fluxes by only considering the advective term U.∇(VCD) (see section 3.5 in Beirle et al., 2023).

Furthermore, the noise of CO2 is probably not critical neither - an outlier pixel causes a high positive and a corresponding negative derivative next to each other, which just cancel out in the spatial integral. Only outliers at the edge of the integration radius might be problematic; this effect can easily be quantified by varying the integration radius.

We agree with the reviewer and mention this in Appendix A. The impact of the edge outliers is indeed mitigated when averaging estimates from different integration radius. Figure R4 illustrates, for example, that the performance of the integral divergence method is improved when averaging estimates across integration radii of 2, 3, and 4 km, compared to using a single radius of 3 km for estimation.

Thus I would like to ask the authors to add a further simple divergence-based emission estimate by just calculating and integrating the divergence on the original (unsmoothed) CO2 data for those days where a plume could be detected, and update all figures accordingly. I consider this to be a fairer comparison to the other methods, and actually expect the divergence method to be competitive to the other methods.

As said above, we have decided not to include single-image estimates of the divergence method in the main method-result sections because we wanted to benchmark the different data-driven inversion methods in their standard version which, for the divergence method, process and generate temporal averaged quantities and because, the recently obtained results, while promising, are preliminary and need to be refined. We have however included some preliminary results in Appendix A concerning the potential of the divergence approach in estimating emissions from single images.

Title: The authors should add "synthetic" before "satellite" in order to avoid misunderstandings.

Corrected as suggested

Line 91: I would propose to have a real enumeration here with new lines for each item.

Corrected as suggested

Line 143: "however the ability of the different approaches to detect unknown point sources has not been studied here"
It might be mentioned that the divergence method is particularly suited for this task.

Following the suggestion of the reviewer, we added the sentence:

Of mention is that the divergence, cross-sectional flux and machine-learning methods are particularly well-suited for automatic detection of plumes from unknown sources (Zheng et al., 2020; Beirle et al., 2021; Schuit et al., 2023)

Line 284: Yes - if the focus is the detection/localization of point sources, temporal averaging is needed. But in this study, the locations are known and assumed as given for all other methods, so they should be considered as given for the divergence approach as well.

As mentioned earlier, temporal averaging helps to identify the enhancements related to CO2 emissions from a specific source in the divergence maps. In most cases, the noise in the observations, spatial variations in the background divergence field, and plumes from other sources make it difficult to distinguish the plume from a particular source in divergence maps derived from single images.

We precise this in the text by rephrasing the sentence:

Old sentence: *Divergence maps are computed from flux fields by using a finite difference approximation and in order to clearly detect point sources, the method needs to average the divergence fields over a long period*

New sentence: *Divergence maps are computed from the mass flux field using a finite difference approximation. Divergence maps are then averaged over a long period to enhance the emission signal, while reducing the impact of noise and the spatio-temporal variations of the CO_2 background*

Table 1: I find the statement that the "Potential for joint use of NO2 to detect plumes" is not given for the divergence method highly misleading.
The divergence does not need to detect a plume - it is based on changes of the flux. But for this, it is of course very helpful to have information on the respective divergence for NO2!

We agree with the reviewer and remove this column from the table as in addition to being misleading, it does not really provide much information.

Generally, the divergence method is the only method capable of localizing a point source without a-priori knowledge, i.e. the NO2 measurements analyzed with the divergence method could build the base for all different methods for CO2 emission estimates by providing the location of point sources.
For the concrete focus of this study, the NO2 divergence might be used as indicator (filter) for favorable (steady state) conditions - if the divergence does not yield reasonable results for NO2, also the CO2 results are probably questionable and should be skipped.

The approach suggested by the reviewer is indeed a good idea, but beyond the scope of this paper. However, we have added a phrase in the conclusion to this effect:

"However, its performance could be improved by selecting and averaging images that are characterized by favorable conditions such as strong signals or wind speeds important enough to guarantee the predominance of advective processes in the atmospheric transport"

We have included below the appendix A that we want to include in the new version of the manuscript:

Appendix A: Potential of the divergence approach to estimate local CO_2 emissions from single-overpass satellite images of XCO_2 and NO_2

In this study, the performance of the divergence approach to estimate local CO_2 emissions from XCO_2 and NO_2 synthetic satellite images is assessed with a standard version of this approach (e.g., Beirle et al., 2021; Hakkarainen et al., 2022), which provides temporally averaged estimates. Results concerning the divergence approach are thus analyzed in the main part of this paper in terms of annual means. However, following the suggestions of a reviewer (S. Beirle), we also tested the potential of this method to estimate instant emissions using single-overpass images. For this purpose, we have used two versions of the divergence approach that have been modified for single image geometry as in Beirle et al. (2023).

For both versions, the computation of the divergence fields is performed by only considering the "advective" term ($10^6 * M_{air} * U * \nabla(VCD)$) of the full expression of the horizontal flux divergence ($\nabla(10^6 M_{air} * U * VCD)$) where M_{air} is the dry air mass, U is the wind vector and VCD is the column in parts per million. Such reformulation of the divergence method that does not compute the divergence of the wind term was also used by Beirle et al. (2023) for NO_2. The advantage of this reformulation for CO_2 is that the background (e.g., a constant offset of 400 ppm) is implicitly removed.

These versions of the divergence approach differ from each other in their way of computing emissions from the divergence maps associated with single-overpass images: the first version integrates the divergence fields on disks centered on the sources (Figure A10). And, to mitigate the impact of the uncertainties in the observations, the emission estimate for a given satellite overpass and source can be computed as the average of the estimates when integrating the divergence signal on disks of different radii. This version of the divergence approach will be referred to hereinafter as the *integral* divergence method. The second version proceeds in a similar way to the one used in the main part of the article and fits a 2-D Gaussian function to the divergence maps in order to retrieve source emissions (e.g. Beirle et al. 2020). The modified peak fitting model is similar to the original but with a reduced number of estimated parameters. Namely, the parameters related to the background and the

location correction (x_0,y_0) are removed from the model parameters. This version of the divergence approach will be referred to hereinafter as the *peak-fitting* divergence method.

For both versions, potential peaks are detected by using NO_2 fields which are integrated over disks of 6 km radius centered on the sources. If the integral of the divergence map on the disk is larger than the integral on the area outside the disk, then the enhancement, related to a given source and for a given satellite overpass, is considered strong enough and the emission estimation can be carried out. Many sources in the SMARTCARB dataset are weak and enhancements may be barely visible which causes challenges for both versions.

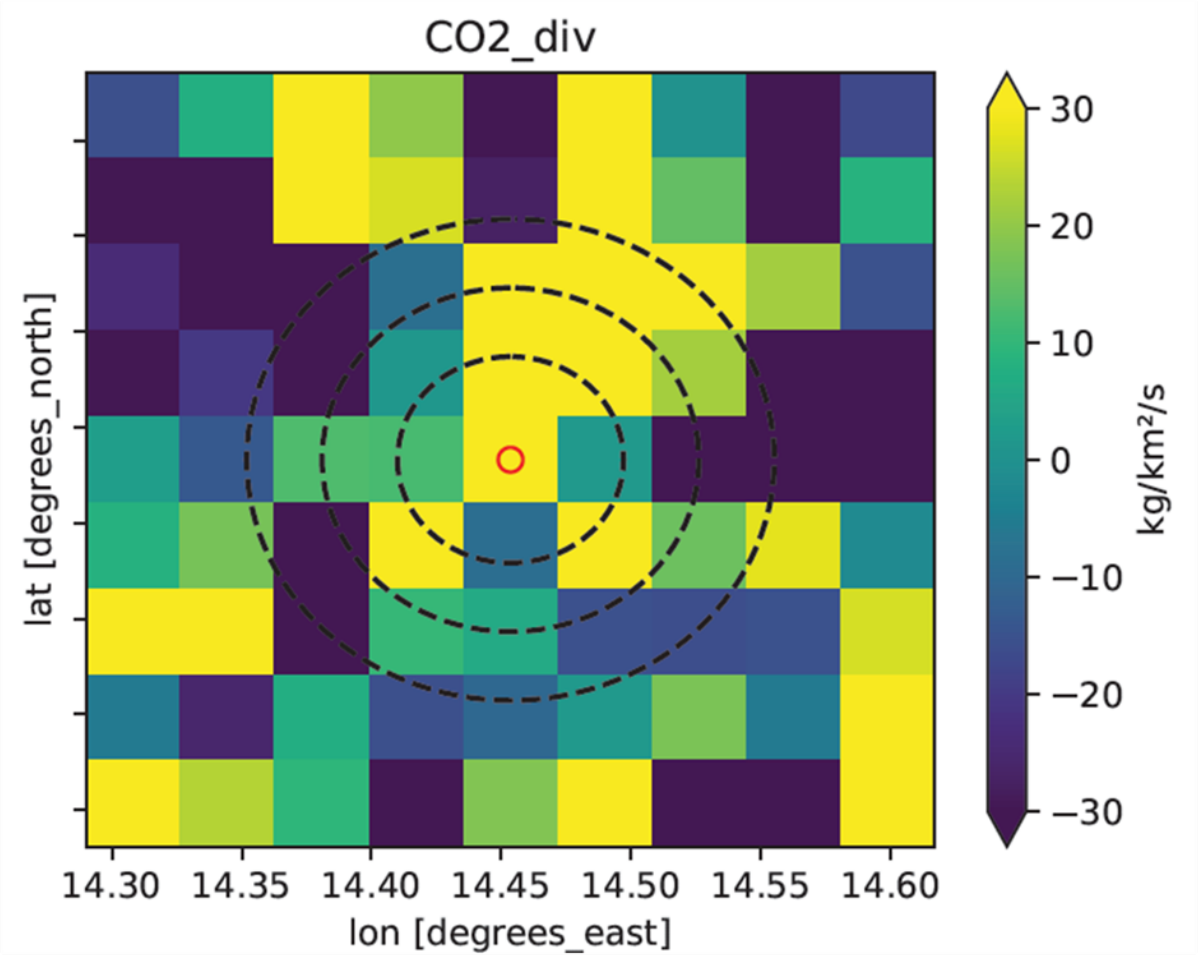

Figure A10: Divergence map estimated around the Janschwalde power station on January 2015 the 12th. Dotted circles show different radii (3 km, 5 km and 7 km) which define integration disks that could be used by the integral divergence method.

To evaluate the potential of these two versions of the divergence approach, we use the SMARTCARB dataset described in section 2.2. which provides about 3000 images to determine the emissions of the 16 local sources that are considered in this study (if we take into account the cloud cover, only 500 images remain usable). Furthermore, we consider two benchmark scenarios (see table 2 and section 2.3) where inversions are performed using CO_2 and NO_2 data with SMARTCARB winds. In one case, we use cloud-free data, while in the other, cloud-filtered data.

The analysis of the deviations from the truth of the instant estimates shows that the integral divergence approach is strongly sensitive to the radius of the integration disks (Fig.

A11). No clear trend appears except that errors increase sharply for a radius greater than 10 km, with a significant presence of outliers. Below this value, the absolute relative deviations (bottom panel of Fig. A11) can increase or decrease depending on the value of the radius Furthermore, the integral divergence approach can underestimate or overestimate emissions depending if the radius is lower or greater than ~4 km. A possible explanation for this behavior could be that the impacts of the two main sources of errors in the divergence method — namely, the uncertainties in the observations and the influence of additional but unwanted sources on the background of the divergence fields — evolve in opposite directions as the integration radius increases. The impact of the uncertainties is mitigated when the area of the integration disk increases because errors have more probability to cancel out. Conversely, the impact of neighboring sources on the background of the divergence field intensifies as the integration radius increases, because the likelihood of capturing features in the divergence maps that are not directly related to the emissions of the targeted sources grows. This impact consistently introduces a positive bias in the estimates (as we capture more sources) and is likely more important than the one related to the uncertainties as performance overall degrades when the integration radius increases.

The peak-fitting divergence method is characterized by a poor performance compared to the integral divergence method for the ensemble of integration radii that we have considered here (Fig. A11). The estimation of small emitting sources may be more difficult for the peak-fitting version as the fit of the 2-D Gaussian function to the data associated to these sources often fails and does not provide optimal and reliable parameter combinations, yielding poor and often overestimated emission estimations. Therefore, even though the peak-fitting divergence method is generally more efficient at the annual scale, these results suggest that it is not the case when estimating instant emissions from single overpass images.

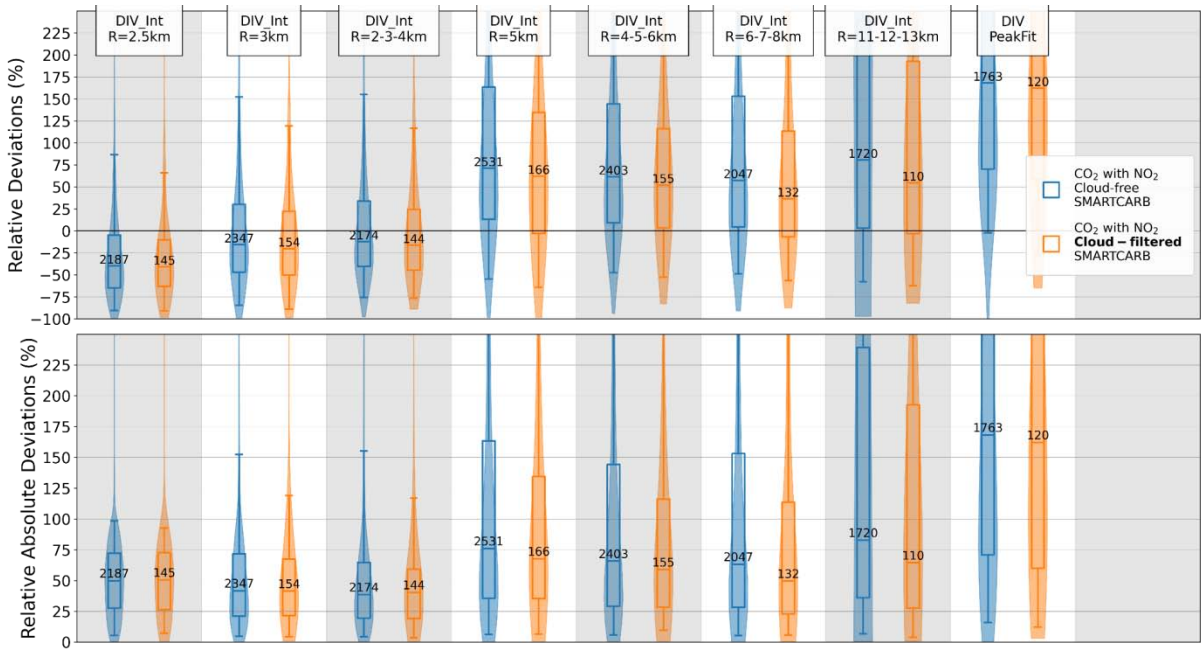

Figure A11: Performances of the different versions of the divergence inversion method when estimating emissions from one year of single images for different benchmarking scenarios: cloud-free CO_2 and NO_2 data with SMARTCARB winds (in blue) and cloud-filtered CO_2 and NO_2 data with SMARTCARB winds (in orange). Distributions of the relative deviations (top panel) and relative absolute deviations (bottom panel) are

illustrated using violin plots. Boxes are the inter-quartiles of the distributions, the whiskers are the 5th and 95th percentiles, and the lines within boxes are the medians. Numbers in the inter-quartile boxes are the number of estimates for each benchmarking scenario and inversion method. Methods DIV_int_R=xkm and DIV_PeakFit are the integral (for an integration radius of x km) and peak-fitting versions of the divergence approach respectively. For a given overpass and source, the emission estimate of the method DIV_int_R=x-y-zkm is the average of the estimates when integrating over circles of x, y and z km radius around the source.

The configuration of the integral divergence method which averages estimates across the integration radii of 2, 3 and 4 km shows the best performance amongst the configurations that we have tested. Probably, the impacts of the data uncertainties and the background are well balanced for this range of radii and the fact of averaging estimates across three different radii further reduces the influence of the data uncertainties on the results. When compared to other inversion methods analyzed in this study, the performance of this configuration of the integral divergence method is similar to that of the best inversion methods (Fig. A12). For the benchmarking scenario considering cloud-free data, its relative absolute deviations are for example characterized by a median value of ~38% and Interquartile Range (IQR) of [~19%–~64%] which are comparable to deviations associated to the Light Cross-Sectional Flux (LCSF) method which have a median value of ~32 % and an IQR of [~15 % – ~56 %]. Note that the integral divergence method generates fewer estimates (2174) compared to the LCSF method (2722), but more than the Gaussian Plume (GP) method (1776).

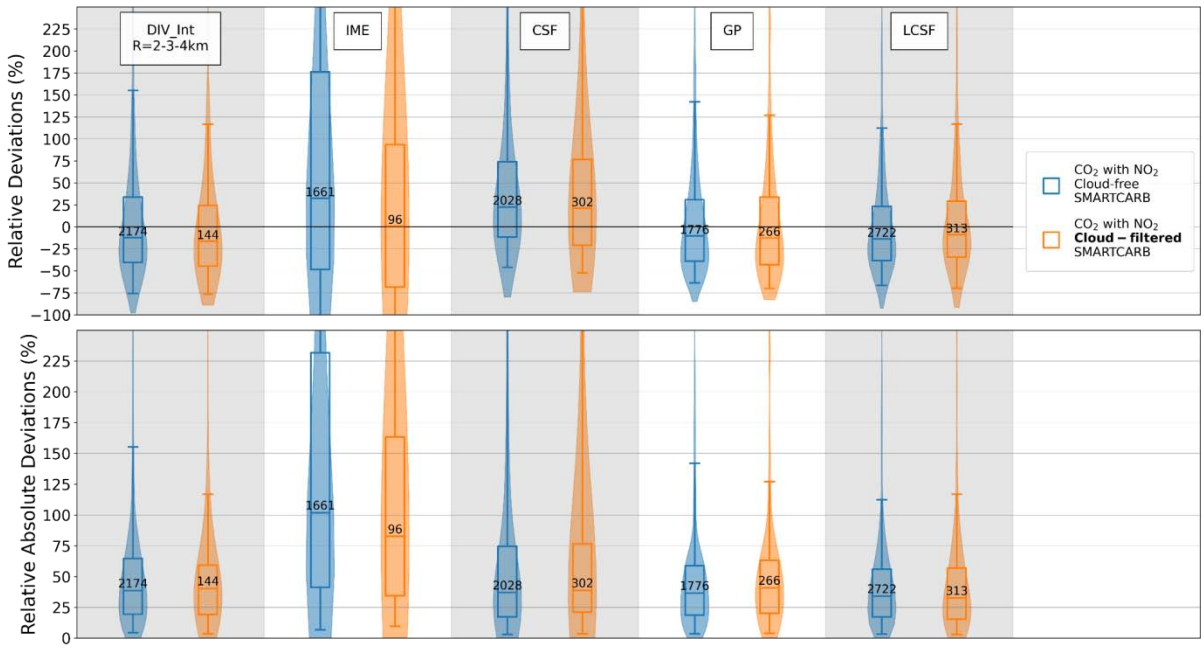

Figure A12: Performances of the inversion methods when estimating emissions from one year of single images for different benchmarking scenarios: cloud-free CO_2 and NO_2 data with SMARTCARB winds (in blue) and cloud-filtered CO_2 and NO_2 data with SMARTCARB winds (in orange). Distributions of the relative deviations (top panel) and relative absolute deviations (bottom panel) are illustrated using violin plots. Boxes are the inter-quartiles of the distributions, the whiskers are the 5th and 95th percentiles, and the lines within boxes are the medians. Numbers in the inter-quartile boxes are the number of estimates for each benchmarking scenario and inversion method. Methods DIV_int_R=2-3-4km and DIV_PeakFit are the integral and peak-fitting versions of the divergence approach respectively. For a given overpass and source, the emission estimate of the method DIV_int_R=2-3-4km is the average of the estimates when integrating over circles of 2,3 and 4 km radius around the source.

These preliminary results regarding the potential of the integral divergence method for estimating local CO_2 emissions from single-overpass images of XCO_2 and NO_2 appear promising, especially since this method allows for the detection of plumes from unknown sources (Beirle et al., 2021). However, further investigation is required to properly assess factors such as the integration radius based on data resolution, and to generalize this method to various types of satellite data. Additionally, a thorough quantitative error assessment is essential to evaluate the accuracy of the estimates, enabling the classification and selection of estimates, which would enhance the method's overall performance.